MICROSCOPIC SHAPE-DEFINED POLYMERIC DEPOTS FOR PROLONGED AND LOCALIZED DELIVERY OF DEXAMETHASONE AND siRNA NANOPARTICLES IN POST-TRAUMATIC OSTEOARTHRITIS

Martina Di Francesco[1], Sean K. Bedingfield[2], Valentina Di Francesco[1], Juan M. Colazo[2], Fang Yu[2], Daniele Di Mascolo[1], Craig Duvall[2], Paolo Decuzzi[1]

[1] Laboratory of Nanotechnology for Precision Medicine, Fondazione Istituto Italiano di Tecnologia (IIT), via Morego 30, Genova, 16163, Italy.
[2] Department of Biomedical Engineering, Vanderbilt University, Nashville, TN 37235, United States.

martina.difrancesco@iit.it

INTRODUCTION

Osteoarthritis (OA) is the most prevalent joint disease and a common cause of pain, functional loss, and disability in older adults. It results from a combination of biomechanical factors and genetic predisposition, affecting the whole joint. In addition to macroscopic features, such as cartilage degradation, subchondral bone remodeling and osteophytes formation, joint capsule hypertrophy, OA is characterized by several cellular and molecular alterations resulting in a chronic low-grade inflammation. Nowadays, there is no treatment for curing this chronic disease by halting or reversing its progression. The only therapeutic options can provide transient relief from the symptoms and allow enhancing temporarily joint mobility and function and joint replacement continues to be ultimately the sole option.

RESULTS

A top-down approach was employed for synthetizing shape-defined PLGA microPlates (μPLs)[1,2] for the sustained release of anti-inflammatory molecules, dexamethasone (DEX) and matrix metalloproteinase 13 (MMP-13) RNA interference nanoparticles (siMMP13-NPs). μPLs, square prims of 20 ×10 μm size, were made out of 15 mg of PLGA (**Fig. 1**).

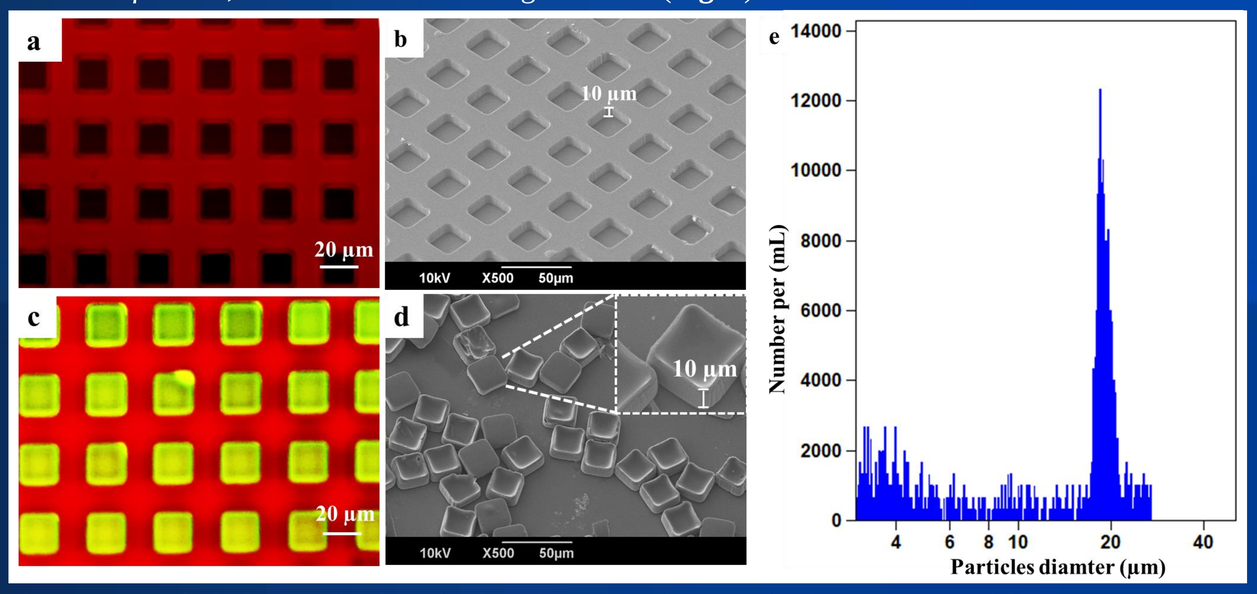

Fig 1. Geometrical characterization of microPlates (μPLs). a. Confocal microscopy and **b.** SEM images of the empty PVA template; **c.** Confocal microscopy image of the PVA template (red) filled with a PLGA/curcumin paste forming CURC – μPLs (green/yellow); **d.** SEM image of μPLs released from the PVA template. The lateral inset shows a magnified and tilted view of the μPLs; **e.** Size characterization of μPLs via Multisizer analysis**.**

μPLs BIOPHARMACEUTICAL CHARACTERIZATION

Also the bio-pharmacological properties of DEX- μPLs were evaluated (**Fig. 2**). The DEX release profile demonstrated a diffusion-driven kinetic with a sustained release for over a week (**Fig.2a** and **b**). μPLs released80% of the payload within the first 10 days (**Fig.2b**), while under confined conditions mimicking the joint capsule, this formulation was able to guarantee a continuous drug release for several months, with ~20% of DEX released in 1 month.

a

Sample	EE%[a]	LE%[b]	DEX per template (μg)	μPL per template	DEX per μPL (pg)
DEX-μPL	12.0 ± 2.5	5.0 ± 0.5	59.2 ± 9.5	24,000 ± 1,500	159.2 ± 19.5

[a]EE% (Entrapment Efficiency); [b]LE% (Loading Efficiency)

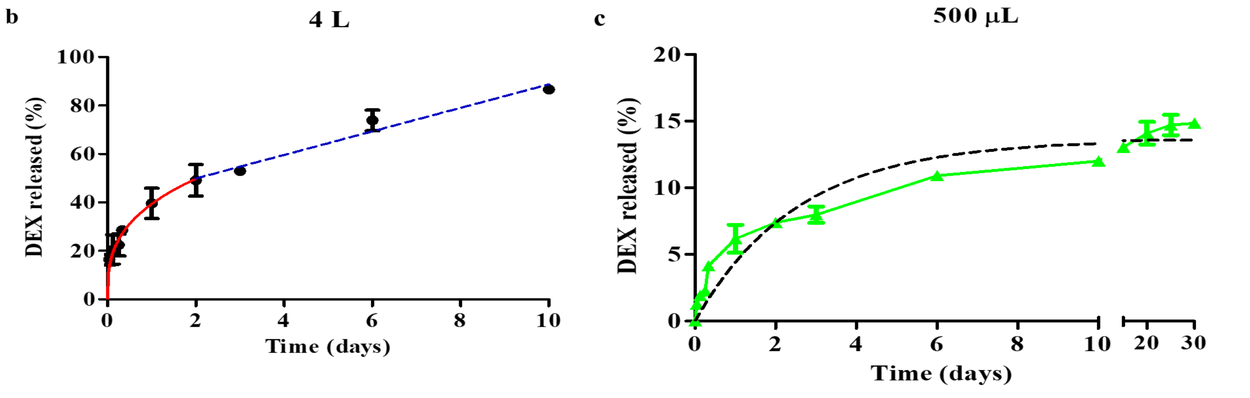

Fig 2. Drug loading and release kinetics of DEX- μPLs. a. DEX-μPL fabrication yield and drug loading characterization; **b.** DEX release profile from μPLs under sink conditions (4 L, red line) and fit to the Weibull empirical drug release model (red line; 95% confidence margin: red margin); **c.** DEX release profile from μPLs under confined conditions, mimicking the synovial volume (500 μL, Weibull: green line with 95% confident band).

μPLs MECHANICAL CHARACTERIZATION

In this configuration, μPLs exhibited a an apparent Young's modulus of ~ 3 MPa value of about of 3.1 ± 0.9 Pa, similar to that of cartilage[3]. Also, they showed a high damping capability (tanδ = 0.3) (**Fig. 3 a** and **b**). This feature can be efficiently used to reproduce the mechanical stiffness of the surrounding micro-environment upon implantation, thus favoring integration and modulating immune responses (**Fig. 3 c**).

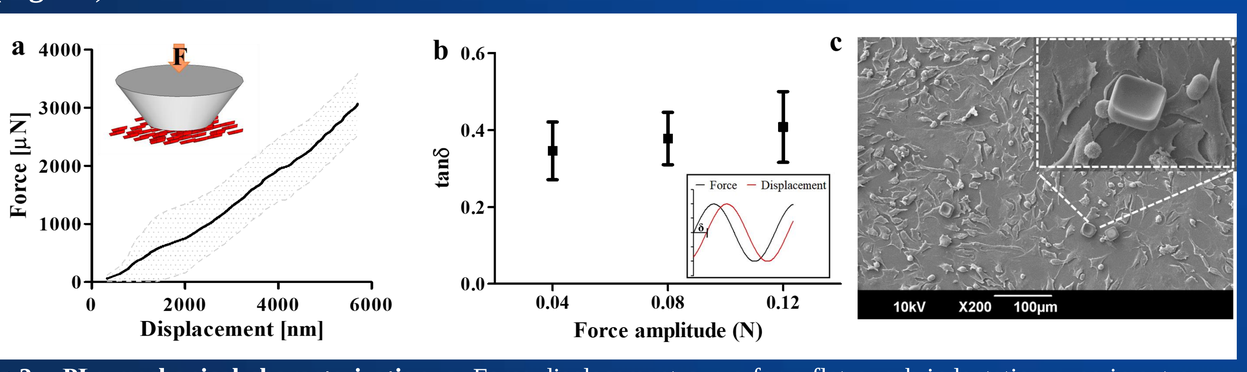

Fig 3. μPLs mechanical characterization. a. Force-displacement curve for a flat punch indentation experiment on an ensemble of μPLs (average curve and standard deviation). In the inset, a schematic of the experimental setup is provided; **b.** Energy dissipation ability of μPL upon cyclic mechanical loading (frequency 5 Hz) as a function of the force oscillation amplitude. In the inset, a schematic of the testing routine is provided highlighting the phase angle δ-dissipation parameter; **c**. 30° tilted view of a SEM image of chondrocytes incubated with μPLs. In the lateral inset, a magnified image shows cells interacting with μPLs;

DEX- μPLs BIOLOGICAL EFFICACY

The anti-inflammatory activity of DEX-loaded μPLs was tested *in vitro* on LPS-stimulated chondrocytes (ATDC5). Results demonstrated that DEX-μPLs reduced the expression of pro-inflammatory cytokines on stimulated ATDC5 at both concentrations tested (**Fig. 4**).

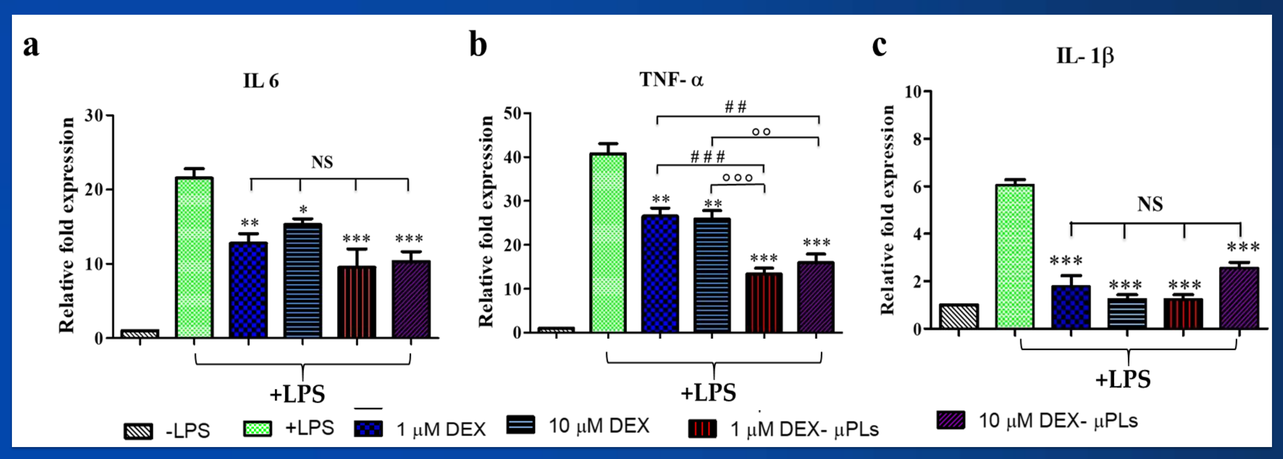

Fig 3. *In vitro* anti-inflammatory effect of DEX-μPLs. a - c . Expression levels of pro-inflammatory cytokines IL-1β, IL-6, and TNF-α for LPS stimulated chondrocytes (ATDC5) cells. (-LPS: no LPS and no μPLs; +LPS: LPS stimulation and no μPLs; DEX: LPS stimulation and free DEX at 1 and 10 μM; DEX-μPLs: LPS treatment and DEX- μPLs at 1 and 10 μM). Results are presented as average ± SD (n = 5). *p< 0.05, **p< 0.001 and ***p< 0.0001 were considered statistically significant as compared to the control (+LPS).

DEX- μPLs *IN VIVO* EFFICACY

At the same time, the therapeutic efficacy of an intra-articular injection of DEX-μPLs in a murine overload injury model was assessed. Results showed that a single injection of DEX-μPLs decreased the expression of IL-1β, TNF-α, IL-6 and MMP-13 by approximately half compared to free DEX at 4 weeks post-treatment. DEX-μPL treatment also reduced load-induced histological changes in the articular cartilage and synovial tissues relative to saline or free DEX treated knees (**Fig. 4**).

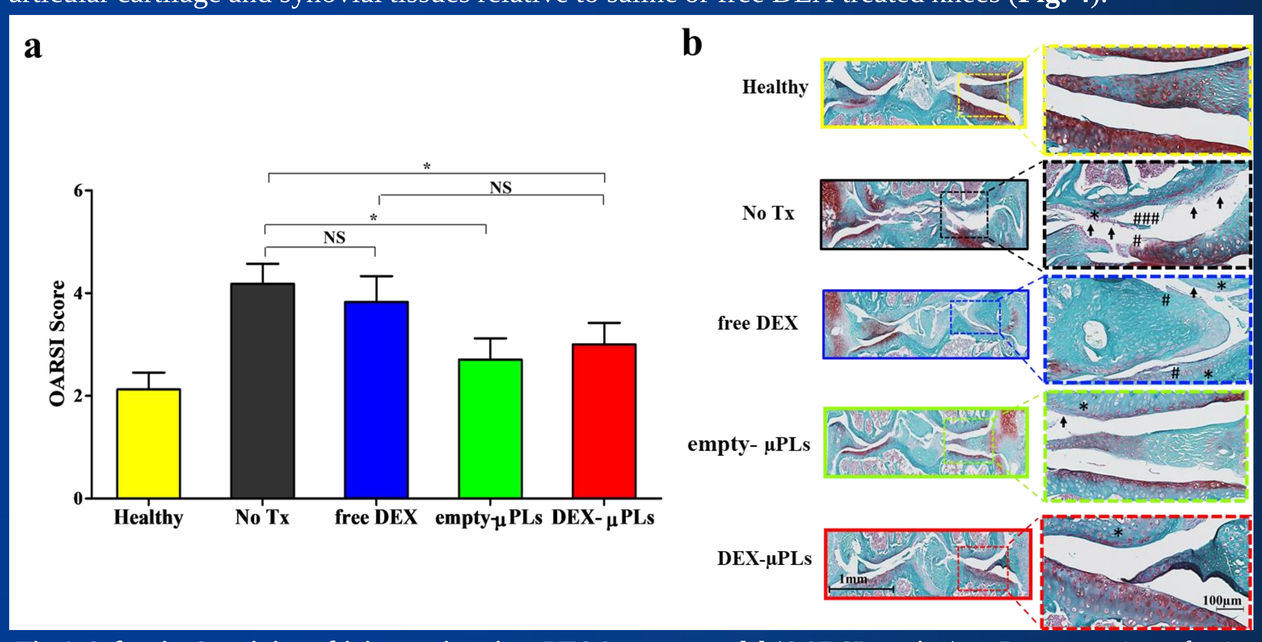

Fig 4. Safranin-O staining of joint sections in a PTOA mouse model (OARSI scoring). a. Representative safranin-O staining of the articular surface of the tibia and femur; inserts show areas of interest under increased magnification; **b.** Blinded histological scoring by OARSI standards. (Histology: Arrows – cartilage erosion, # - cartilage fissures, * - low safranin-O staining.

siMMP13-NPs- μPLs PRELIMINARY CHARACTERIZATION

Finally, siMMP13-NPs were efficiently loaded inside μPLs. At the same time, gene silencing efficiency was obtained by siMMP13-NPs released from μPLs for the whole duration of the study (5 weeks), preserving ~50% silencing after 4 weeks

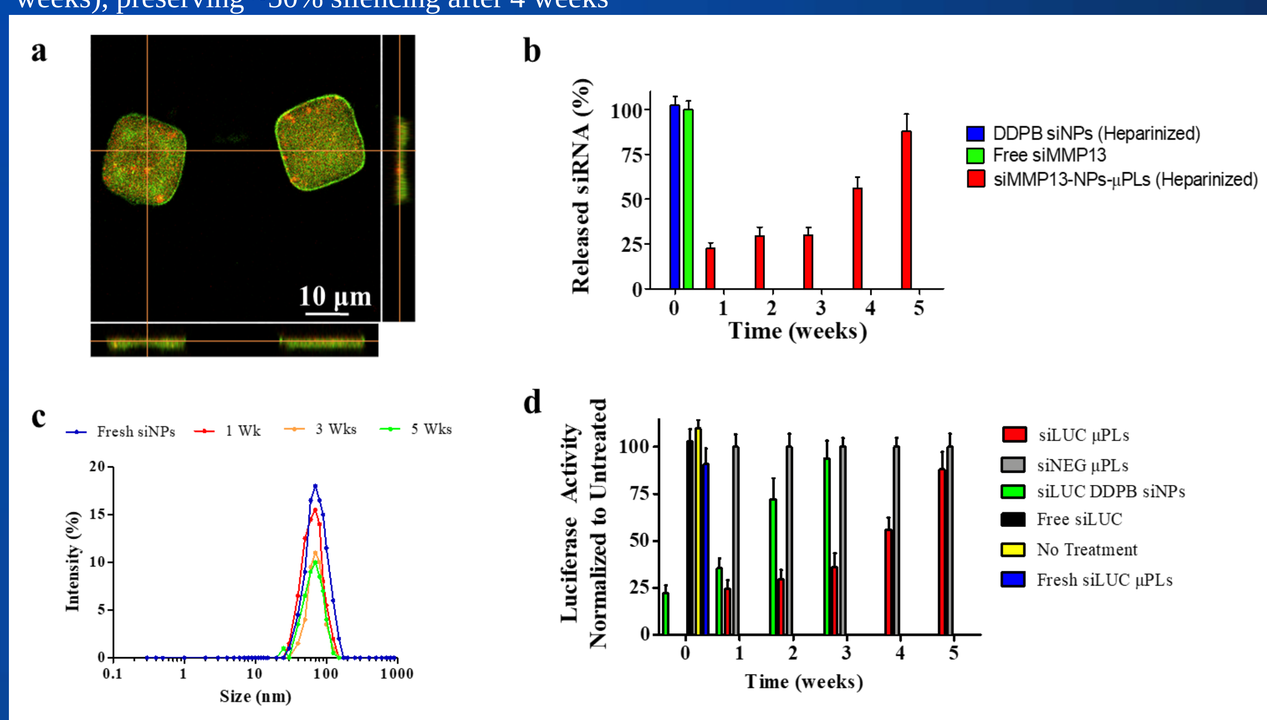

Fig 5. Phsico-chemical and biopharmaceutical characterization of siRNA-NPs loaded μPLs. a. 2D confocal microscopy image of CURC – μPLs (green/yellow) loaded Cy5-DNA-NPs (red); **b**. siMMP13 release profile from μPLs under confined condition (1.5 mL)**; c.** Average size of siMMP13 nanoparticles release in the medium; **d.** Anti-luciferase siRNA particles activity released from μPLs on LUC+ chondrocytes (ATDC5).

CONCLUSIONS

Top-down fabrication strategy allowed us to synthetize shaped-defined μPLs ensuring a sustained drug release for several weeks, to alleviate pain, inflammation, and favor tissue regeneration, and mechanical support of the joint, to minimize wear, cartilage laceration and improper bone remodeling.

REFERENCES

1. Di Francesco et al., *ACS applied materials & interfaces*, **2018**. 10(11): p. 9280-9289.
2. Di Francesco et al., *Journal of Controlled Release*, **2020**. 319: p. 201-212.
3. Mansour, *Biomechanics of cartilage. Kinesiology: the mechanics and pathomechanics of human movement*, 2003: p. 66-79.